

Half-life of the rp -process waiting point nucleus ^{84}Mo

J. B. Stoker^{*1,2}, P. F. Mantica^{1,2}, D. Bazin², A. Becerril^{2,3,4}, J. S. Berryman^{1,2}, H. L. Crawford^{1,2}, A. Estrade^{2,3,4}, C. J. Guess^{2,3,4}, G. W. Hitt^{2,3,4}, G. Lorusso^{2,3,4}, M. Matos^{2,4}, K. Minamisono², F. Montes^{2,4}, J. Pereira², G. Perdikakis², H. Schatz^{2,3,4}, K. Smith^{2,3,4}, R. G. T. Zegers^{2,3,4}

⁽¹⁾ *Department of Chemistry, Michigan State University, East Lansing, Michigan 48824*

⁽²⁾ *National Superconducting Cyclotron Laboratory, Michigan State University, East Lansing, Michigan 48824*

⁽³⁾ *Department of Physics and Astronomy, Michigan State University, East Lansing, Michigan 48824*

⁽⁴⁾ *Joint Institute for Nuclear Astrophysics, Michigan State University, East Lansing, Michigan 48824*

Email: stoker@nscl.msu.edu

The half-life of ^{84}Mo , an even-even $N = Z$ nucleus near the proton dripline created during explosive hydrogen burning in Type I X-ray bursts in the rapid proton capture (rp) process, was remeasured and found to be more than 1σ shorter than the previously adopted value. The effect of the measured half-life on rp -process reaction flow is explored.

*10th Symposium on Nuclei in the Cosmos
July 27 - August 1 2008
Mackinac Island, Michigan, USA*

*Speaker.

1. Introduction

The observed abundances for the p -nuclei $^{92,94}\text{Mo}$ and $^{96,98}\text{Ru}$ are currently at odds with abundance predictions from established solar production mechanisms [1]. The rp -process, which is a sequence of (p, γ) reactions and subsequent β^+ decays that starts at the seed nucleus ^{41}Sc and terminates at $^{107,108}\text{Te}$ [2], can produce these nuclei under certain circumstances. The amount of rp -process material emitted into the interstellar medium depends on the isotopic overproduction factor, the frequency of X-ray burst occurrences that produce p -nuclei, and the fraction of material that escapes the gravitational field of the neutron star [3]. The high gravitational field in the vicinity of neutron stars hinders stellar ejection of all but the most energetic ash [4] during X-ray bursts. Therefore, the bulk of nuclei synthesized in the rp -process is not expected to escape the gravitational field. Nevertheless, the amount of ejected material is still being debated and the composition of material produced in an rp -process event relies on experimental data, including β -decay half-lives that govern the overall mass processing rate and the composition of the ash.

We have remeasured the half-life of ^{84}Mo , an rp -process waiting point nucleus. The half-life of ^{84}Mo is a necessary experimental parameter for modeling reaction flow above $A = 84$, and directly determines the amount of ^{84}Sr formed during X-ray bursts. The previously adopted half-life value of $3.7_{-0.8}^{+1.0}$ s [5, 6] was not determined to high precision, and is at odds with theoretical expectations [7, 8].

2. Experimental Procedure

^{84}Mo was produced at National Superconducting Cyclotron Laboratory by fragmentation of a primary beam of ^{124}Xe at energy 140 MeV/nucleon in a 305 mg/cm^2 ^9Be target. The desired fragments were selected with the A1900 Fragment Separator [9] with a 180 mg/cm^2 Al wedge and 1% momentum slit at the intermediate image of the device. Further secondary beam separation was accomplished with the Radio Frequency Fragment Separator (RFFS) [10]. The RFFS was operated

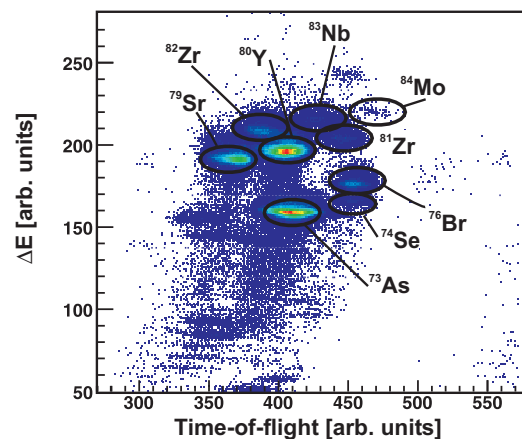


Figure 1: Particle identification plot for ^{84}Mo fragments. The overall rate of ions after the RFFS was 0.5 Hz. The ΔE signal was obtained from the most upstream Si PIN detector of the BCS. Time-of-flight was determined between the same Si PIN detector and the cyclotron radiofrequency.

at $V_{pp} = 47$ kV and a frequency of 23.145 MHz, matched to the K1200 cyclotron. Unwanted ions were removed from the beam by a 10 mm vertical slit placed ~ 3 m downstream of the RFFS. The particle identification spectrum after separation in the RFFS is depicted in Fig. 1.

The experimental apparatus consisted of a combined setup of the NSCL β Counting Station (BCS) [11] and 16 Ge detectors from the Segmented Germanium Array [12]. The BCS was used for event-by-event correlation of fragment implantations with their subsequent β decays. The central detector of the BCS was a Double-Sided Silicon Strip Detector (DSSD) of dimensions $4\text{ cm} \times 4\text{ cm} \times 995\text{ }\mu\text{m}$ thick. The DSSD was segmented into 40 1-mm strips in both the x and y dimension, providing 1600 individual pixels. The high degree of DSSD segmentation and beam filtering from the RFFS were crucial to realize an average time between implantations into a single pixel that exceeded the correlation time, which was set in software to be 10 s based on the previously-determined half-life of ^{84}Mo . The efficiency for β detection was $\approx 38\%$ considering correlations between an implantation in a given pixel and a subsequent decay within the same pixel or the four nearest neighbor pixels.

3. Results and Discussion

The decay curve for β -decay events correlated with ^{84}Mo implantations is presented in Fig. 2. These data were fitted based on the maximization of a Poisson probability log-likelihood function that considered the exponential decay of the ^{84}Mo parent, the exponential growth and decay of the

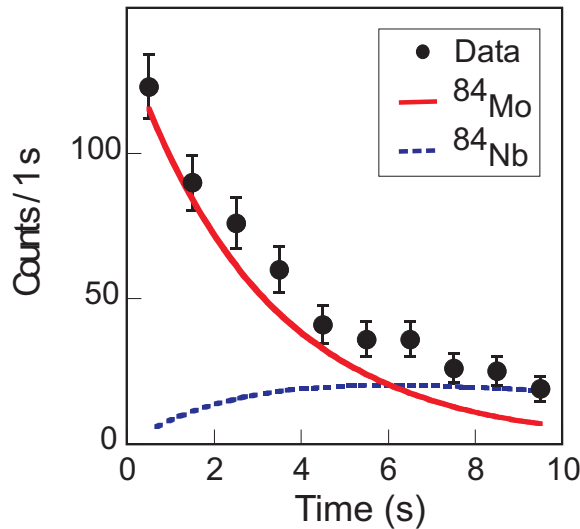


Figure 2: Decay curve for β decays correlated to ^{84}Mo implantations within a 10 s time window. A preliminary half-life of 2.0 ± 0.4 s for ^{84}Mo was deduced from the fit. The fit was determined through the maximization of a Poisson distribution log-likelihood function that considered contributions from the exponential decay of the ^{84}Mo parent, the exponential growth and decay of the ^{84}Nb daughter, and a linear background. A fixed value of 9.5 s for the daughter half-life was provided for the fit. The data are summed into 1 s bins, represented by the black circles in the plot. The parent and daughter components of the fit are represented by the solid and dashed lines, respectively. The background contribution to the fit is not shown.

^{84}Nb daughter with a known half-life of 9.5 s [13], and a linear background. A preliminary half-life of 2.0 ± 0.4 s was deduced based on a sample size representing 1037 ^{84}Mo implantations.

A shortcoming in the above fitting procedure is that all decay times were considered to be independent, which does not accurately describe the probability density of daughter decays. A maximum likelihood analysis is underway to improve the precision of the ^{84}Mo half-life result.

The new preliminary half-life of ^{84}Mo is more than 1σ shorter than the previous value of $3.7_{-0.8}^{+1.0}$ s [5]. We note that the sample size in the measurement reported here is nearly 30 times larger than that realized in Ref. [5]. The new half-life value is found to be consistent with the QRPA results of Sarriguren *et al.* [7], who properly accounted for the ground state deformation parameters of neighboring nuclei.

The implications of the new half-life value of ^{84}Mo on the *rp*-process abundances for the $A = 84$ mass chain were calculated using a single zone X-ray burst model based on REACLIB-V1 rates [14]. The abundance with respect to burst duration is shown in Fig. 3 for ^{84}Mo (solid lines) and for all $A = 84$ isobars (dashed line). The shaded region covers the range of previously predicted half-lives ($0.8 \text{ s} \leq T_{1/2} \leq 6.0 \text{ s}$) given by various models [7, 8, 15]. The dot-dashed line represents the yield calculated using the experimental upper limit of 4.7 s taken from the previously-measured half-life of ^{84}Mo . The order of magnitude uncertainty in the final ^{84}Sr abundance is reduced to less than a factor of two with the new and more precise half-life.

4. Acknowledgments

The authors thank the NSCL operations staff for providing the primary and secondary beams for this experiment and NSCL γ group for assistance setting up the Ge detectors from SeGA. We

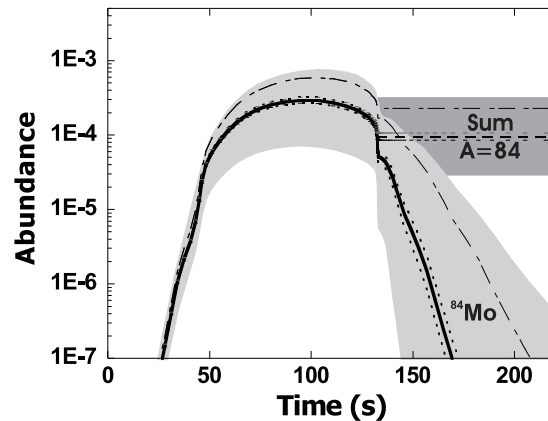


Figure 3: Impact of ^{84}Mo half-life on the final $A = 84$ isobar abundance. Abundance is reported as a ratio of (mass fraction)/(mass number). Time 0 corresponds to the hydrogen-ignition start time. The solid line, bounded above and below with dotted uncertainties, shows the result using the newly-measured ^{84}Mo half-life. The dashed line corresponds to summed abundance of all $A = 84$ isobars. The dot-dashed line represents the yield calculated using the experimental upper limit of 4.7 s taken from the previously adopted half-life of $3.7_{-0.8}^{+1.0}$ s for ^{84}Mo from Ref. [5]. The shaded regions highlight the range in abundance based on the full range of theoretical half-lives.

are appreciative of insightful statistics discussions with G.F. Grinyer and J. Thorpe. This work was supported in part by the National Science Foundation Grants PHY-06-06007, PHY-05-20930, and PHY-02-16783.

References

- [1] V. Costa, M. Rayet, R.A. Zappalia, and M. Arnould, *Astron. Astrophys.* **358**, L67 (2000).
- [2] H. Schatz, *Nucl. Phys.* **A746**, 347c (2004).
- [3] R.N. Boyd, *Eur. Phys. J. A* **13**, 203 (2002).
- [4] N. Weinberg, L. Bildstein, and H. Schatz, *Astrophys. J.* **639**, 1018 (2006).
- [5] P. Kienle, T. Faestermann, J. Friese, H.-J. Korner, M. Munch, R. Schneider, A. Stolz, E. Wefers, H. Geissel, G. Münzenberg, C. Schlegel, K. Summerer, H. Weick, M. Hellström, and P. Thirolf, *Prog. Part. Nucl. Phys.* **46**, 73 (2001)
- [6] T. Faestermann, R. Schneider, A. Stolz, K. Summerer, E. Wefers, J. Friese, H. Geissel, M. Hellström, P. Kienle, J.J. Korner, M. Mineva, M. Munch, G. Münzenberg, C. Schlegel, K. Schmidt, P. Thirolf, H. Weick, and K. Zeitelhack, *Eur. Phys. J. A* **15**, 185 (2002).
- [7] P. Sarriguren, R. Alvarez-Rodriguez, and E. Moya de Guerra, *Eur. Phys. J. A* **24**, 193 (2005).
- [8] G.T. Biehle and P. Vogel, *Phys. Rev. C* **46**, 1555 (1992).
- [9] D.J. Morrissey, B.M. Sherrill, M. Steiner, A. Stolz, and I. Wiedenhoöver, *Nucl. Instrum. Methods Phys. Res. B* **204**, 90 (2003).
- [10] D. Gorelov, V. Andreev, D. Bazin, M. Doleans, T. Grimm, F. Marti, J. Vincent, and X. Wu, *Proceedings of the 2005 Particle Accelerator Conference*, ed. C. Horak, p. 3880 (2005).
- [11] J.I. Prisciandaro, A.C. Morton, and P.F. Mantica, *Nucl. Instrum. Methods Phys. Res. A* **505**, 140 (2003).
- [12] W.F. Mueller, J.A. Church, T. Glasmacher, D. Gutknecht, G. Hackman, P.G. Hansen, Z. Hu, K.L. Miller, and P. Quinn, *Nucl. Instrum. Methods Phys. Res. A* **466**, 492 (2001)
- [13] J. Doring, A. Aprahamian, R.C. de Haan, J. Gorres, H. Schatz, M. Wiescher, W.B. Walters, L.T. Brown, C.N. Davids, C.J. Lister, and D. Seweryniak, *Phys. Rev. C* **59**, 59 (1999).
- [14] JINA Reaction Library Database REACLIB-V1, <http://www.nsl.msui.edu/~nero/db>
- [15] K. Takahashi and K. Yokoi, *Nucl. Phys.* **A404**, 578 (1983).